Available online at www.sciencedirect.com
ScienceDirect
Journal of Power Sources 170 (2007) 308–323
JOURNAL OF POWER SOURCES
www.elsevier.com/locate/jpowsour

Review

Thermal plasma spraying for SOFCs: Applications, potential advantages, and challenges

Rob Hui [a], Zhenwei Wang [a,*], Olivera Kesler [a,b], Lars Rose [a,c], Jasna Jankovic [a], Sing Yick [a], Radenka Maric [a], Dave Ghosh [a]

[a] *National Research Council Institute for Fuel Cell Innovation, 4250 Wesbrook Mall, Vancouver, BC V6T 1W5, Canada*
[b] *Department of Mechanical Engineering, University of British Columbia, 2054-6250 Applied Science Lane, Vancouver, BC V6T 1Z4, Canada*
[c] *Department of Materials Engineering, University of British Columbia, 309-6350 Stores Road, Vancouver, BC V6T 1Z4, Canada*

Received 23 February 2007; accepted 29 March 2007
Available online 18 April 2007

Abstract

In this article, the applications, potential advantages, and challenges of thermal plasma spray (PS) processing for nanopowder production and cell fabrication of solid oxide fuel cells (SOFCs) are reviewed. PS processing creates sufficiently high temperatures to melt all materials fed into the plasma. The heated material can either be quenched into oxide powders or deposited as coatings. This technique has been applied to directly deposit functional layers as well as nanopowder for SOFCs application. In particularly, low melting point and highly active electrodes can be directly fabricated on zirconia-based electrolytes. This is a simple processing technique that does not require the use of organic solvents, offering the opportunity for flexible adjustment of process parameters, and significant time saving in production of the cell and cost reduction compared with tape casting, screen printing and sintering processing steps. Most importantly, PS processing shows strong potential to enable the deposition of metal-supported SOFCs through the integrated fabrication of membrane-electrode assemblies (MEA) on porous metallic substrates with consecutive deposition steps. On the other hand, the application of PS processing to produce SOFCs faces some challenges, such as insufficient porosity of the electrodes, the difficulty of obtaining a thin (<10 μm) and dense electrolyte layer. Fed with H_2 as the fuel gas and oxygen as the oxidant gas, the plasma sprayed cell reached high power densities of 770 mW cm^{-2} at 900 °C and 430 mW cm^{-2} at 800 °C at a cell voltage of 0.7 V.

Keywords: Solid oxide fuel cells; Thermal plasma spraying; Nanopowder; Components; Integrated fabrication; Cost reduction

Contents

* Corresponding author. Tel.: +1 604 221 3111; fax: +1 604 221 3001.
E-mail address: Zhenwei.Wang@nrc-cnrc.gc.ca (Z. Wang).

0378-7753/$ – see front matter © 2007 Published by Elsevier B.V.
doi:10.1016/j.jpowsour.2007.03.075

1. Introduction

Solid oxide fuel cells (SOFCs) are highly efficient devices that can convert fuel electrochemically to electricity, with negligible pollution emissions [1]. SOFCs have the potential to oxidize a wide range of readily available fuels, including renewable biomass fuels such as alcohols, and hydrocarbons such as natural gas. Consequently, they are an obvious choice for more efficient utilization of existing energy resources. They can be used for electrical power and heat generation with low environmental pollution and greenhouse gas emissions [2]. However, there are some challenges still to be overcome before widespread commercialization of SOFCs will take place, primarily involving the high costs of materials, manufacturing, and systems as well as insufficient reliability and durability of the stacks.

PS processing is a well established and proven technology, which is already in widespread industrial use for a variety of applications due to the low cost and simplicity of the processes. For example, PS processing can deposit thermal barrier coatings (TBCs) to insulate metallic components of diesel engines or gas turbines so that they can be operated more efficiently at higher temperatures, with increased resistance to oxidation [3]. PS processing is also used for the manufacture of coatings to improve wear resistance and mechanical properties [4]. Although significant challenges remain in the development and implementation of PS processing for the production of SOFCs, substantial potential exists for both cost and performance benefits, compared to the use of traditional wet ceramic processing techniques. In this review, the advantages of PS processing and its application for production of powders, functional components, and integrated SOFC layers are summarized, and the potential advantages and challenges of PS processing for SOFC fabrication are presented.

2. Principle of plasma

The PS process is an industrially well-established line-of-sight surface coating technique that was developed in the 1960s [5]. The technique utilizes plasma created by high-voltage electrodes to partially or fully melt particles that traverse the plasma jet and are deposited on a substrate [6]. Anode nozzle exit velocities are typically on the order of 900–2000 m s^{-1} [7,8]. Plasma jet temperatures generally vary between 7000 K and 20,000 K [9]. Consequently, all known inorganic materials can be deposited, as the melting temperatures T_m all lie below the plasma jet temperature. Due to the high-process temperatures, materials with a small (<300 K) difference between T_m and the vaporization temperature T_{vap} or decomposition temperature T_d tend to vaporize or decompose, leading to low deposition efficiencies [10]. Low deposition efficiencies can result from high vaporization rates of the deposited materials, from material rebound, which occurs when the particles have only partially melted or resolidified prior to impact, or from the parameters of the deposition. The deposition efficiency decreases with an increase in plume spread or with rotation of a planar sample holder. The spraying distance and the jet velocity affect the residence time in the plasma, which determines whether the materials have been sufficiently melted before reaching the substrate, or are already resolidified, leading to rebound.

If the particles have resolidified prior to impact, they will mostly bounce off the surface. If they have decomposed or evaporated, they never reach the surface. If they are still liquid, they impact on the surface, where they flatten to form a splat by spreading at a rate of about 15–25 m s^{-1} [11]. Cooling rates greatly depend on the substrate heat conduction and surface topography, and lie in the range of 10^6 K s^{-1} to 10^7 K s^{-1}, similar to the rates achieved in liquid quenching [11,12]. Coatings are formed by the consecutive build-up of impacting coating material splats [13]. Fig. 1 depicts the splat formation and also gives an indication of the average time needed for each process [10]. The rate of layer deposition is mainly determined by the time it takes for subsequent splats to impact on a surface.

The process is a line-of-sight process. Consequently, complex geometric shapes can be difficult to coat, or may require specialized robots as an operator. Substrate holder rotations can only ease these restrictions to a limited degree. Since coatings are applied layer by layer, there is no limitation to the substrate area, and the procedure is easy to scale up compared to wet ceramic processing.

Standard plasma gases are N_2, H_2, Ar, and He and combinations thereof. The differences in gas energy density at different temperatures stem from the properties of the gases. For example, hydrogen and nitrogen dissociate at relatively low temperatures. Whereas helium does not ionize below 13,000 K, nitrogen undergoes dissociation and ionization at approximately 10,000 K. At 13,000 K, nitrogen can supply about six times more energy than an equal volume of helium. In the case of dissociating molecules, large amounts of energy can be supplied by re-association of the molecules without significant changes in temperature.

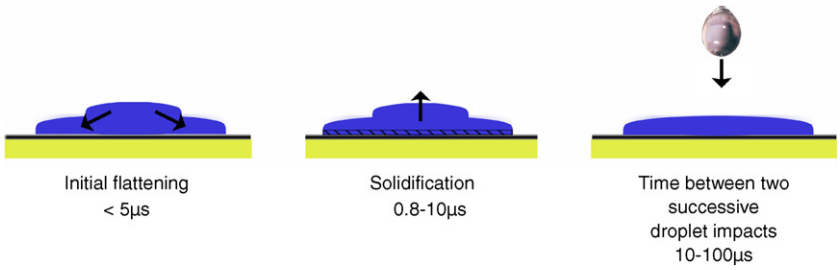

Fig. 1. Splat impact and solidification on a substrate, with the time each process takes on average [8] (with reproduction permission from Professor Fauchais).

Diatomic nitrogen dissociates into free atoms:

$$N_2 + \text{energy} \rightarrow 2N \quad (1)$$

With further increase in energy input, the gas ionizes:

$$2N + \text{energy} \rightarrow 2N^+ + 2e^- \quad (2)$$

The reverse process provides the energy for heating the coating material during spraying:

$$2N^+ + 2e^- \rightarrow 2N + \text{energy} \rightarrow N_2 + \text{energy} \quad (3)$$

Reversible dissociation of diatomic gases results in higher energy content per volume when compared to monoatomic gases. Consequently, they have a lower plasma temperature, but can much more readily transfer the energy to particles traveling through the plasma.

In order to start the plasma in the torch, the gas must be ionized. This is done by applying a voltage to the gas. Above a certain breakthrough voltage, electrons are extracted from the atomic core and the gas becomes ionized. The more energy necessary for the first ionization of an atom, the more difficult it is to start the plasma, and the higher the breakthrough voltage.

Nitrogen is one of the main gases used in thermal plasma spraying. It is the cheapest of the four standard PS gases, and is generally inert, except when sprayed with nitridization sensitive materials such as Ti alloys [14]. It readily absorbs energy, with the potential to transfer that energy to the feedstock as described in Eq. (3). The plasma color of nitrogen is yellow, and the first ionization energy is 14.53 eV.

Argon is the most used primary plasma and shroud gas. It is a noble gas, and inert to all spray materials. Argon creates relatively low temperature plasmas. It is used either solely or in mixtures with other gases to increase its energy and has low heat conductivity. Argon is the easiest gas to form plasma, and tends to be less aggressive on the spray equipment, electrodes and nozzles than either nitrogen or hydrogen. For that reason, most plasma torches are started using pure argon, and then the composition of the plasma gas is changed as required. Pure Ar has a blue plasma color, and a first ionization energy of 15.75 eV.

Hydrogen is mainly used as a secondary gas, usually to a maximum of 20 vol.%. It increases heat conduction even in low concentrations (<5 vol.%) and acts as an anti-oxidant. Pure hydrogen produces a red plasma and has an ionization energy of 13.60 eV.

Helium is also mainly used as a secondary gas. Being a noble gas, it is inert to all spray materials and is used when hydrogen or nitrogen additions have disadvantageous effects. Like hydrogen, helium possesses good heat conduction. It is commonly used for high-velocity plasma spraying of high-quality carbide coatings, for which process conditions are critical. However, it is also the least abundant gas and the most expensive. It is usually only used if there are chemical reactions between hydrogen and the feedstock material. The first ionization energy is the highest of all elements, 24.58 eV.

3. Nanopowder synthesis for SOFCs

3.1. Nanopowders for SOFCs

Current developmental targets for SOFCs include increased volumetric power density, lower operating temperature, increased reliability and durability, and reduced cost. In response to these goals, the need for materials with improved physical and mechanical properties for demanding applications is becoming increasingly apparent. Advances in powder-based processing have been focused on reducing particle size and improving the particle uniformity. Nano-scale powders, approximately 1–100 nm in size, are becoming increasingly critical to the innovations in numerous applications, including catalysis, coatings, cosmetics, electronics, sensors, and drug delivery.

Nanopowders offer controlled functionality, increased reactivity, and a number of other advantages over coarser materials, such as higher surface area, catalytic activity, and sinterability. Prospects for further commercialization into diverse areas such as automotive and aerospace components and textiles are also excellent, although these applications currently form a relatively small market for nanopowders [15]. New powder production methods promise to further improve the capabilities to control particle morphologies and minimize particle sizes.

Nanomaterials in particular are of considerable interest for use in SOFCs due to their potential to increase the surface area of active sites on which the electrode reactions take place, thereby improving reaction kinetics. There is a demand to decrease the SOFC operation temperature in order to improve the system reliability, durability, and cost. One problem created by reduced operation temperature is the decreased electrode reaction rate, which may result in large polarization losses. SOFC electrode reactions occur mainly at the interfaces between phases that conduct oxygen ions, gases, and electrons, commonly referred to as triple-phase-boundaries (TPBs). Therefore, an extended reaction surface area with an optimized porous microstructure will enhance the electrode performance. Mixed ionic and electronic

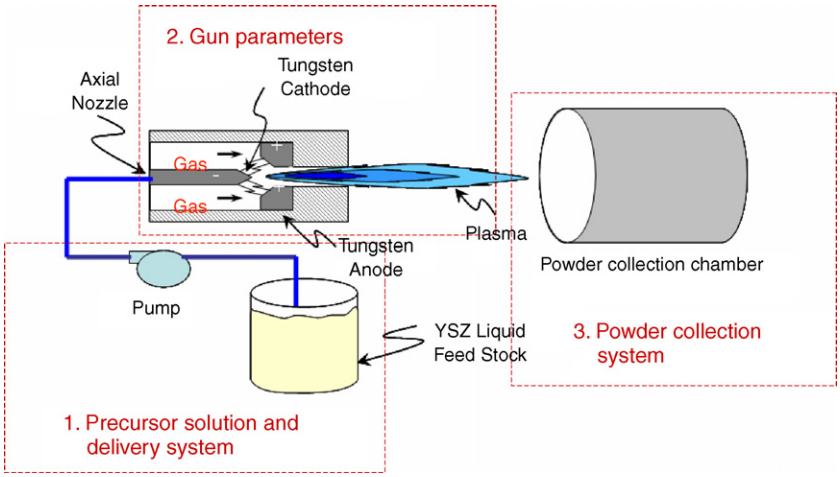

Fig. 2. Schematic diagram of a plasma spray system for nanopowder synthesis.

conductors (MIECs) can be used to enlarge the reaction surfaces to the entire electrode particle surface, thus significantly improving the electrode reaction kinetics [16]. In addition, nanomaterials with dimensions down to the atomic scale (10^{-9} m) represent a new generation of advanced materials with improved physical, chemical and mechanical properties [17,18]. A feature of such nanomaterials is the high fraction of atoms that reside at grain boundaries and grain surfaces, largely enhancing the chemical activity. Nanostructured materials provide unprecedented opportunities for significantly improved materials performance [19–22]. Nanostructured materials also have the enhanced electrical conductivity that is required for SOFC components, either ionic or electronic conductivity [23]. Nanoscale electrolyte powders can be sintered at decreased temperatures [24] compared with micron-scaled powder to avoid the chemical reactions between different components at high-sintering temperatures. Such lowered sintering temperatures are of great importance for the one-step sintering fabrication of an entire single cell [25]. Moreover, low sintering temperature leaves more porosity and more active sites (higher surface area), which accelerates gas diffusion and electrochemical reactions on TPBs. Nanopowders are expected to facilitate thin-film deposition of dense electrolyte layers to decrease ohmic losses and polarization losses.

3.2. Nano-powder production by PS processing

PS processing has inherent advantages in the production of advanced materials in the form of coating of powders. Plasma techniques offer a controllable and directional heat source. Plasma temperatures are much higher than achievable by using fossil fuel combustion, and are sufficiently high to melt or dissociate any compounds fed into the plasma, to melt or vaporize virtually all elements, and to potentially allow the reactions between feedstock materials to take place in the gas phase. These high temperatures, along with the chemically reactive species formed in the plasma, may accelerate chemical reactions by several orders of magnitude. Residence time in the high-temperature zone is short and controllable. The ability to quench rapidly from very high temperatures produces very small spherical particles, typically a few tens of nanometers to a few hundred nanometers in diameter. By a suitable choice of plasma environments, reactions can take place in an inert atmosphere, or a suitable oxidizing, reducing, or other reactive environment. Starting materials can be fed into the plasma reactors in gaseous, solution, suspension, and powder form. Generally, reactants should be chosen to avoid the production of corrosive or toxic by products, e.g., metals can be fed as oxides or nitrates rather than chlorides.

Generally speaking, PS processing for nanopowder production includes the following components as shown in Fig. 2:

1. *Precursor feedstock and delivery system.*
2. *Plasma forming and spraying system*: plasma forming, plasma gas injection nozzle, mixtures of Ar, He, N_2, or H_2 as described in Section 1, plasma reaction, plasma outlet.
3. *Powder collection system*: nucleation, particle growth, and filters, cyclones, or cooled surfaces for particle separation from the material flow stream.

These synthesis steps are much simplified compared to conventional wet chemical routes. The cost is therefore expected to be competitive. Different materials including metals, ceramics, and composites have been prepared using plasma technology. The capability of plasma processing to fabricate nanostructured materials has been attracting interest [26–28]. This technique has recently been employed as an alternative processing route for SOFC fabrication, including component deposition and powder production. Several researchers have carried out experiments to fabricate SOFC components by plasma spraying, and established its usefulness as a fuel cell fabrication process [29–45]. Table 1 lists some selected nanopowders for SOFC applications. It can be seen that the costs for nanopowders from n Gimat Co. (former MicroCoating Technologies) using a spray process in conjunction with a flame method, are lower than those resulting from the non-spray-based methods used at Fuel Cell Materials.

More recently, there has been an increased interest in using PS methods for the synthesis of nanostructured ceramic powder materials. Some laboratories have demonstrated the feasibility

Table 1
Price comparison of selected nanopowders for SOFCs

Powder	Average particle size (nm)	Price (US$ kg^{-1})	Manufacturer	Technology
Yttria-stabilized zirconia (YSZ)	50–80	2295	Fuel Cell Materials	Unknown
	<50	1200	n Gimat Co.	Combustion chemical vapor deposition
	50–100	2000	TAL Materials	Flame spray pyrolysis
$La_{1-x}Sr_xMnO_3$ (LSM)	1200	665	Fuel Cell Materials	Unknown
	<50	On request	n Gimat Co.	Combustion chemical vapor deposition

of synthesizing nanopowders directly from liquid precursors, such as SUNY Stony Brook [46] and NanoProducts Corporation (NPC) [32,33,47]. The researchers found that crystalline structure of zirconia changed from tetragonal to monoclinic when the particle size increased, thus demonstrating a potential use of nanopowder production techniques to control material properties other than particle size [46]. NPC has successfully synthesized <20 nm powders from precursor solutions, including cerium oxide, zirconium silicon oxide, zinc oxide, high-purity aluminum oxide, copper oxide, and magnesium oxide. NPC claims that their process has been fully scaled to tonnes per month quantities with cost-effective prices. Tekna Plasma Systems Inc. has licensed from Nanosource Technologies for the production and commercialization of TiO_2 nanopowders.

US Nanocorp has also synthesized SOFC powders by plasma spray processing [48]. Fig. 3 shows XRD spectra of $La_{0.4}Ce_{0.6}O_{2-\delta}$ (LDC40) nanopowder synthesized by PS and compared with that of the powder prepared by a wet chemical route [48]. No obvious difference can be found. In contrast, the XRD pattern in Fig. 4 of plasma sprayed Sr- and Mg-doped $LaGaO_3$ (LSGM) powder shows that the powder is not a single phase, even after heat-treatments at different temperatures. The undesired phases in the LSGM powder from PS processing are the same as those observed in powder prepared using a wet chemical route and annealed at 1000 °C, indicating that the reaction was not completed during the plasma processing or the wet chemical processing. The melting point of MgO is approximately 2800 °C, which makes it more difficult to be dissolved into the final solid solution than other dopants with lower melting temperatures. Higher energy plasma conditions may be required to melt all the component materials in plasma synthesis. Further process improvement is therefore necessary for the preparation of single phase LSGM powder. Northwest Mettech Corp. and Institute of Fuel Cell Innovation (NRC-IFCI) are developing a plasma spraying system for nano powder production. Fig. 5

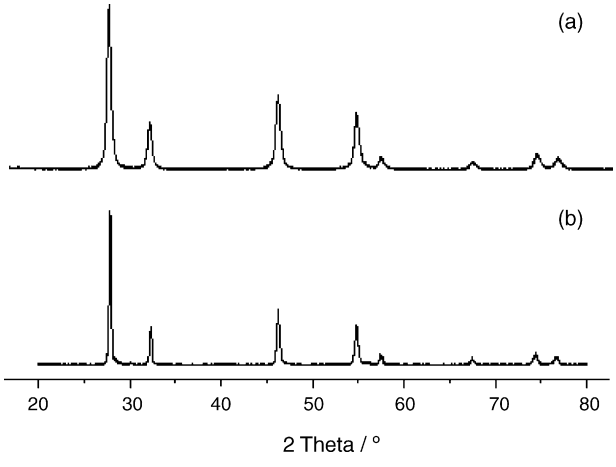

Fig. 3. XRD patterns of $La_{0.4}Ce_{0.6}O_{2-\delta}$ powders produced by (a) plasma spray processing and (b) wet chemical synthesis [48].

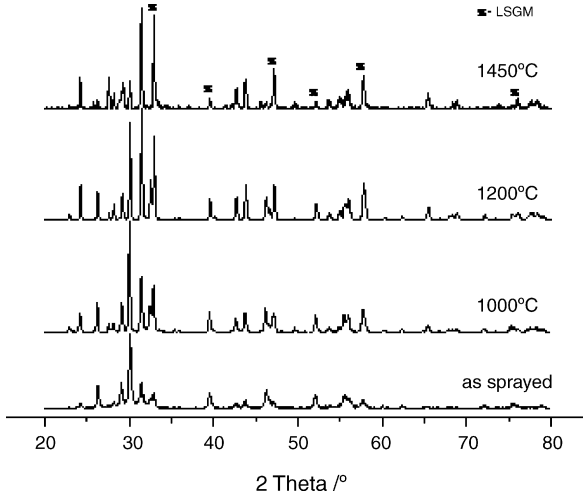

Fig. 4. XRD patterns of LSGM powders plasma sprayed and calcined at different temperatures [48].

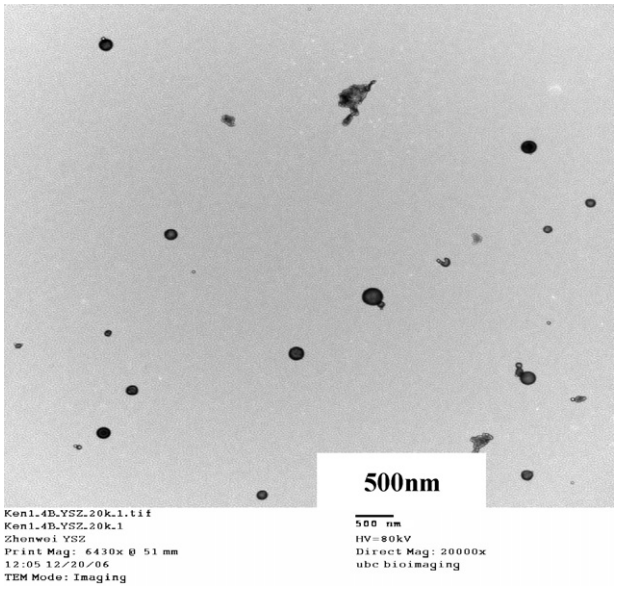

Fig. 5. TEM photo of plasma sprayed YSZ powder [49].

gives the TEM photo of as-sprayed 8 mol% yttria stabilized zirconia (8YSZ) powder [49]. The YSZ powder shows mostly spherical with mean size of about 200 nm. Compared with the application of PS for SOFC fabrication, efforts directed at using plasma spraying for powder production are still very limited so far.

4. Fabrication of SOFCs

4.1. Advantages of plasma spray processing

Traditional wet ceramic techniques based on tape casting, screen printing, and co-sintering of layers are the state of the art processing methods for the fabrication of SOFC single cells, and therefore widely adopted and intensively investigated. However, traditional wet ceramic techniques face several problems that include but are not limited to the following items:

(1) Multiple separate instruments, such as an extruder or tape-caster, screen-printer, and one or more furnaces are required for the multiple steps of the wet ceramic technique.
(2) High-temperature firing leads to a substantial and rapid increase in capital costs as the volume of cell production increases due to the long processing time and the need for enlarging production rates through the use of parallel production lines. Approximately 1 day is required for each firing cycle, in addition to the drying time required after each wet deposition process prior to the fabrication of subsequent layers. Even for cells in which the anode, electrolyte, and cathode are all co-fired in one step, the throughput of the process is limited by the time required to ramp the deposited layers to and from a high-sintering temperature and hold them there for sufficient densification times, or by the availability of multiple large firing kilns.
(3) The size enlargement of single cells to more than 15 cm × 15 cm creates serious problems resulting from large total shrinkage or thermal expansion mismatch strain, often leading to macro-cracks, severe warping, or cell fracture during high-temperature firing steps.
(4) High-temperature firing steps lead to inter-reactions between adjacent cell layers. For example, highly active $Ln_{1-x}Sr_xCo_{1-y}Fe_yO_{3-\delta}$ (Ln = La, Gd, Sm, Pr, etc.) cathodes react with zirconia-based electrolytes, forming insulating layers [50], and nickel in Ni anodes reacts with lanthanum strontium magnesium gallate (LSGM) electrolytes to form non-conductive layers [51].
(5) Some novel anode materials for direct hydrocarbon oxidation, such as those utilizing copper as an electronically conducting phase, cannot be sintered at the high temperatures required for electrolyte densification (1300–1450 °C) due to low melting temperatures, resulting in the impossibility of co-firing the electrolyte together with these electrode materials.
(6) High-temperature sintering generally precludes the use of metallic interconnect layers as the structural support for the SOFCs, unless impurities are added to lower the electrolyte sintering temperature, which can negatively impact performance, and inert, vacuum, or reducing atmospheres are used during firing, which substantially increases the process cost.

In contrast, PS processing potentially provides a much simplified and cost-effective choice for fabricating SOFC components and integrated cells. Low melting point and highly active electrode materials can be deposited directly onto zirconia-based electrolytes without detrimental inter-reaction. PS processing allows the entire multilayer SOFC to be processed in a consecutive spray process using only one piece of equipment and within a few minutes. PS processing also has the ability to achieve considerably higher deposition rates than those obtained through conventional physical or chemical vapor deposition techniques. Moreover, PS processing is easily scaled up in terms of individual cell size and volume of production. Plasma spraying is also of potential interest for the improved control of composition, porosity, and microstructure within the electrodes because functionally graded and consecutively adjusted microstructures can be easily deposited, which are difficult to realize using wet ceramic processing [52].

4.2. Anode fabrication

Generally speaking, coatings deposited by plasma spraying have a porosity ranging from 5 vol.% to 15 vol.%, which is much less than the desired porosity level of approximately 40 vol.% required for high-gas diffusivity within SOFC anodes. Additional porosity is produced during NiO reduction to Ni, which generally elevates the porosity by approximately 20 vol.%, depending on the NiO content in the anode precursor. Moreover, anode layers can be directly fabricated on porous metal supported structures with a thickness as low as 20 μm, so that the lower porosity is less likely to seriously deteriorate the electrochemical performance of the sprayed cell, compared to anode supported cells.

PS processing facilitates the deposition of graded layers with changes in composition or microstructure as a function of distance across the deposited layer. Traditional wet ceramic techniques can deposit only discrete layers of a fixed composition and powder particle size distribution. Therefore, if a spatial variation in microstructure and composition is desired, multiple depositions of discrete layers must be performed to obtain the functionally graded electrodes, by utilizing a series of different slurry feedstocks. In contrast, PS processing can introduce compositional gradients in microstructure in a coated layer by spraying the two components from separate reservoirs, and gradually changing the relative amounts of each as the coating is deposited [53]. Moreover, both the porosity and particle surface areas can be controlled during deposition in order to obtain microstructures ranging from a high-reaction surface area and TPB length near the electrode-electrolyte interfaces to a higher porosity near the electrode-interconnect boundary. These microstructural gradients can be achieved during deposition by varying the spray parameters while building the layers, or by changing to a different feedstock reservoir with different powder particle size distributions during spraying. Additionally, higher electronic conductivity phases for current collection can

be deposited at higher volume fractions towards the electrode-interconnect boundary. Such compositional gradients have been shown previously to significantly reduce thermal stresses caused by the changes in operating temperatures, relative to the thermal stresses present at the sharp interface between two adjacent but dissimilar materials [53].

This advantage shows particular potential in the production of direct oxidation anodes based on Cu-rare-earth element doped ceria (RDC) and Ru/Pd-RDC material systems, due to the higher thermal expansion coefficients and the differential shrinkage character of those material combinations compared to standard NiO–YSZ anodes. Currently, such anodes must be manufactured with an even more complex processing procedure than that is typically used for SOFCs, usually including repeated infiltrations and calcinations. As a result, even more processing steps have to be used to manufacture these anodes by the infiltration of a previously sintered porous anode pre-form [54]. In addition to requiring a larger number of processing steps, this technique also provides less control over the anode microstructure than conventional wet ceramic techniques. PS processing dramatically simplifies the manufacturing process for these anode layers, with or without small quantities of an additional catalyst material, such as Co [44].

Electron-conducting oxides, such as $La_{1-x}Sr_xCr_{1-x}Mn_xO_{3-\delta}$ (LSCM), are regarded as promising alternatives for anode materials for direct hydrocarbon electrocatalytic oxidation [55]. During co-firing at the temperature range of 1300–1450 °C, LSCM shows much less shrinkage than the YSZ electrolyte, resulting in high porosity and poor interfacial bonding with the electrolyte layer, which leads to high-interfacial resistance and polarization losses. Meanwhile, LSCM tends to chemically react with YSZ, as do other advanced perovskite electrode materials. Atmospheric PS (APS) has been used to deposit (La, Sr)$CrO_{3-\delta}$ anode materials on YSZ substrates [56], which suggests that PS may have the potential to fabricate LSCM layers on metallic supports or on YSZ electrolytes with suitable porosity and good interfacial bonding.

Plasma spraying has also been used to fabricate anodes in tubular cathode-supported SOFCs [57–59], including spraying performed in atmospheric conditions. It has been suggested that for tubular cells, PS processing may be too complex and therefore expensive to implement, despite the potential advantages described in Section 3.1 [60]. However, this assessment was based on a manufacturing process that included PS as one of several steps, including high-temperature firing steps, and so the primary cost and material advantages of PS, resulting from eliminating high-temperature sintering steps altogether, was not realized when combining PS with additional wet ceramic and firing steps rather than replacing those steps with a fabrication process based entirely or primarily on PS. On the other hand, a PS-based process, when combined only with low-temperature firing steps that do not exceed inter-reaction temperatures of the component materials nor rapid oxidation temperatures of metallic interconnect supports, may also provide some benefits even though additional processing steps may be required in that case [61].

4.3. Electrolyte fabrication

Co-sintering of electrolyte and electrodes is usually limited by high-temperature reactions between perovskite electrodes and cubic zirconia-based electrolytes, or between nickel in anodes and LSGM-based electrolytes. Due to the elimination of high-temperature firing, PS processing offers a rapid and cost-effective method to fabricate electrolytes directly on various electrode materials, with all of the layers supported on metallic interconnect substrates.

Moreover, electrolyte layers can be plasma sprayed on cathode-supported tubular SOFCs conveniently, thus eliminating high-temperature sintering steps which would otherwise lead to inter-reactions between the electrolyte and cathode [58–60]. Conventional atmospheric plasma spray processing, however, results in porous and lamellar microstructures (5–15% porosity), which in turn result in low open circuit voltage and cell efficiency or in the need to produce thick electrolytes to minimize open porosity. Deposition of electrolytes has therefore sometimes been followed by post-deposition heat treatments in order to further densify the coatings, including calcining steps and spark plasma sintering treatments [33,62,63]. Various processing improvements are currently being developed to obtain more homogenous, denser, and thinner electrolytes through the use of fine powders, slurry spraying, or reduced pressure during spraying, in order to minimize or eliminate the need for post-deposition heat treatments.

4.3.1. Atmospheric plasma spraying of electrolytes

Atmospheric plasma spraying (APS) has been widely investigated for the production of dense electrolyte layers [29,32,33,62,64–70]. It is difficult to fabricate dense electrolyte layers by single-step deposition by PS. Although some post-deposition heat treatments, such as spark plasma sintering [62], high-temperature vacuum sintering [66], and chemical impregnation densification [61,67], can improve the electrolyte density and alleviate the gas leakage, these post-spraying treatments increase the process complexity. For example, high-temperature vacuum sintering requires a complex furnace and firing at a temperature as high as 2000 °C, while the impregnation densification generally requires repeated cycles of wet coating, drying, and firing.

Another major challenge in the development of dense electrolytes through APS is the avoidance of cracks, typically generated during the spraying process [64]. The major influencing factors are the particle properties in the plasma jet, the substrate temperature, the movement of the gun during deposition, the particle size distribution of the feedstock powder, and the powder feeding rate. The spray gun used can also play a major role.

Siemens Westinghouse Power Corporation recently has been trying to replace the electrochemical vapor deposition process by less expensive APS processing in tubular cells [71]. Cylindrical and flat tubular SOFCs with a high-power density (HPD) design are currently produced mainly by APS. The state of the art materials used in tubular and HPD SOFCs and their respective manufacturing processes are listed in Table 2 [71].

Table 2
Main raw materials and processing techniques used in Siemens Westinghouse SOFC fabrication [71]

No.	Components	Materials	Processes
1	Cathode	Doped $LaMnO_3$	Extruded and sintered
2	Interlayer	Various	Slurry coating
3	Interconnection	Doped $LaCrO_3$	APS process
4	Electrolyte	Yttria stabilized zirconia	APS process
5	Anode	Ni–YSZ	APS process

Further efforts are required to obtain higher open circuit voltages, reduction of operation temperatures, and improvements in cell performance.

LSGM electrolytes have also been deposited on tubular LSM substrates by APS. LSM tubes used as SOFC cell support layers generally have high porosity, and were found to have low thermal shock resistance, and cracked when exposed to a plasma flame [71]. Through experimental optimization, this substrate cracking or melting problem was eventually solved, obtaining electrolyte densities ranging from 93% to 96%, and cell open circuit voltages (OCV) of approximately 1.0 V [71]. The LSGM coating was approximately 200 μm in thickness and well bonded to the tube with no visible cracks. As shown in Fig. 6a [71], the coating is dense and well adhered to the tube substrate. There are still some closed pores in the coating. The electrolyte layer shows some cracks with a typical length of 10–20 μm (Fig. 6b [71]), which results in a slightly decreased OCV, requiring a thicker layer for gas tightness. Thicker electrolyte layers, however, result in lower cell performance due to higher series resistance. The cracks are not interconnected, and are believed to be caused by overheating. The amount of micro-cracking can potentially be reduced to an acceptable extent by further process optimization.

Fig. 7 shows the crystalline structure of a sprayed LSGM electrolyte. Small amounts of amorphous oxides exist in the electrolyte layer as sprayed, and then disappear after post-deposition heat treatment at 800 °C [33]. This temperature is much lower than the densification temperatures of traditional ceramic processing and, in practice, can be carried out during cell testing or operation.

4.3.2. Suspension plasma spraying of electrolytes

In order to improve flowability, dry electrolyte powders are often fed as large particles with sizes ranging from approximately 20–120 μm. Some of these large particles cannot be completely melted, which results in electrolyte layers thicker than 50 μm with some pores and cracks. Suspension plasma spraying (SPS) is an emerging technology that utilizes a liquid feedstock carrier, permitting the projection of much finer initial feedstock, and allowing the formation of thinner coatings [41,72,73]. In this process, a feed suspension is injected directly into the plasma flame. The plasma–liquid interaction atomizes the suspension into a fine mist and evaporates the suspension medium, thereby concentrating the solid content into micro-sized particles [74,75]. The small particles are nearly immediately accelerated to plasma gas velocity. At impact on the substrate, the particles form thin lamellae with rapid solidifi-

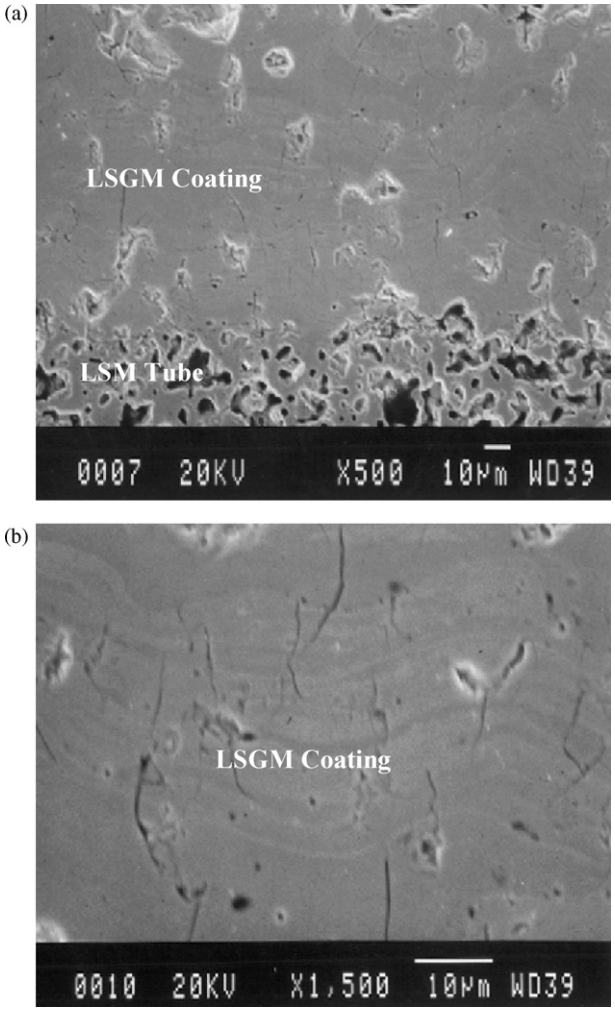

Fig. 6. Cross-section of an LSGM coating on an LSM tube: (a) 500× magnification and (b) 1500× magnification [48].

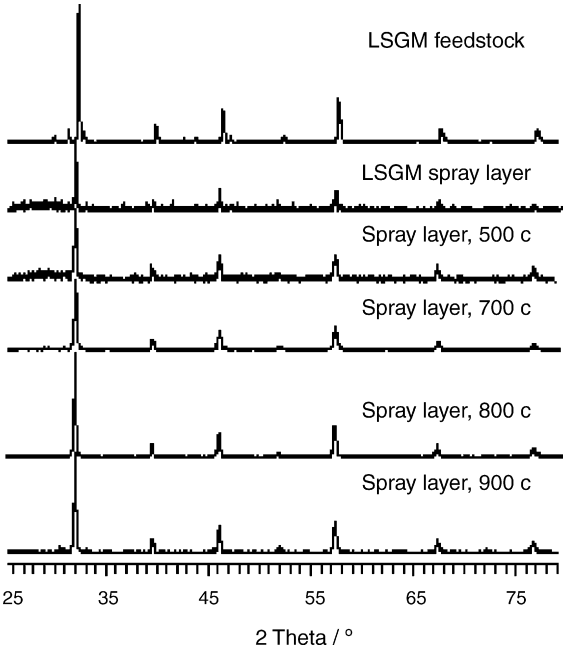

Fig. 7. XRD patterns of feedstock and plasma sprayed LSGM electrolyte material heat treated at different temperatures [33].

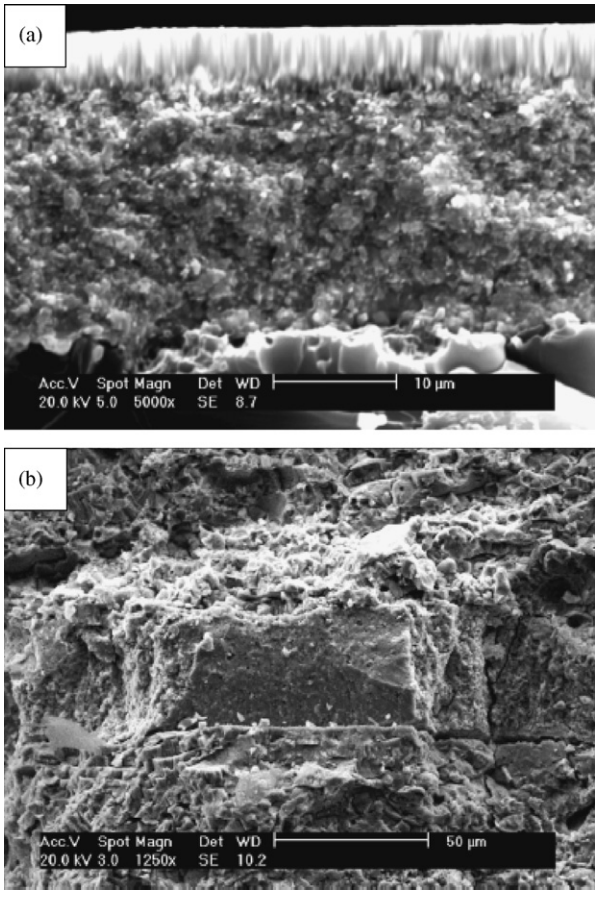

Fig. 8. SEM micrograph of YSZ coatings plasma sprayed in an air atmosphere [72]. (a) SPS; (b) traditional APS. (With reproduction permission from IEEE Intellectual Property Rights Office).

cation rates. With a lower solid content of the suspensions, more electrolyte particles are completely molten, and a denser coating can be deposited. By adjustment of the process conditions, SPS processing offers the possibility to control the coating thickness and microstructure. Thin electrolyte layers with 3–20 μm thickness and more refined microstructure than that achieved with powder APS can be obtained. Fig. 8 compares SEM images of YSZ coatings obtained by SPS and by traditional APS. The coating made by SPS processing is much more homogeneous and no splat stacking can be observed, in contrast to the traditional PS coating, where the presence of a layered splat structure is visible [72]. SPS processing can also be used for the preparation of $LaMnO_3$ perovskite-based cathodes [76].

4.3.3. Small particle plasma spraying of electrolytes

Small-particle plasma spraying (SPPS) is another evolving method that allows the deposition of thin and dense electrolyte coatings [77,78]. SPPS is a modified APS technique in which a beveled injector allows particles as small as 200 nm to be entrained into the outer shell of the plasma jet and efficiently deposited onto a substrate. The melting point of the electrolyte powder, spray distance, total plasma gas flow rate, composition of hydrogen in the plasma gas, injector offset, injector angle, and carrier gas flow rate can all play an important role in microstructural control. Through the use of fine powders, SPPS can produce dense YSZ coatings (>98%) with thickness as thin as 5 μm [78]. SPS and SPPS are still relatively novel techniques, and have not been widely applied for SOFC fabrication.

4.3.4. Vacuum plasma spraying of electrolytes

Because pressures as low as 50 mPa reduce the interaction of molten particles with surrounding cold gases, thin-films produced by vacuum plasma spraying (VPS) typically possess higher density than those manufactured by APS, and exhibit better substrate adhesion. Additionally, the plasma jet plume is less turbulent in VPS, and particle speed reduction from nozzle to substrate is less pronounced. Therefore, the reproducibility of the resulting layers is improved. Hence, VPS is often used for fabricating SOFC electrolytes, where high density, small thickness, and flatness are primary requirements. The VPS process can also be adjusted to produce porous NiO/YSZ coatings with up to 15% porosity. However, capital and operating cost exceed that of atmospheric plasma spraying by approximately one order of magnitude. Creating vacuum conditions prior to every deposition run and during spraying with a high-gas flow rate makes this batch processing technique less favorable economically. Nonetheless, continuous processing can be achieved by even higher capital investments to install pre-vacuum chambers and a continuous line of production. VPS applications are discussed in more detail in Section 4.

4.4. Cathode fabrication

In wet ceramic processing techniques, some highly active cathodes for intermediate- and low-temperature SOFCs, such as (La, Sr)(Co, Fe)$O_{3-\delta}$ (LSCF), cannot be fired in contact with zirconia electrolytes due to the appearance of $La_2Zr_2O_7$ and $SrZrO_3$ impurities during the firing at high temperature (>1000 °C) [79,80]. Insertion of a protective interlayer between cathode and electrolyte further increases the complexity of cell structure, but successfully prevents inter-reaction between cobalt-containing cathodes and YSZ electrolytes. In processing conditions where a high-temperature firing step is required to densify the electrolyte, protective interlayers may be used to prevent inter-reaction between the cathode and electrolyte layers [81].

However, PS eliminates the need for high-temperature sintering steps entirely, and thus enables the application of highly active cathodes such as lanthanum strontium cobaltite (LSC) to zirconia-based electrolytes [63] with no additional interlayer required. During PS processing, the molten particles in the high-temperature plasma flame are quenched down to temperatures below 500 °C at rates of close to 10^6 K s^{-1}, sufficiently rapidly so that no diffusion-based reactions can take place between the sprayed coating layer and the substrate. This benefit leads to the potential for improving cell performance while also simplifying manufacturing procedures and lowering cost, particularly in the development of reduced temperature SOFCs that operate below 700 °C. Below that temperature, high-performance cathodes are particularly beneficial, so avoiding their inter-reaction with the fuel cell electrolyte layer becomes particularly important.

In traditional wet ceramic processing, highly specialized electrode powders with suitable phase structure and fine particle size and inks with suitable viscosity are preconditions to obtaining high-oxygen reduction activity in the electrode. In the case of PS processing, however, a much wider range of precursors, such as perovskite powders [82], liquid mixtures of metal carbonates and metal nitrates [83], suspensions [84], or nitrate solutions [85], can all be adopted as spraying precursors. In order to obtain suitable electrode microstructures, pre-processing such as suspension formation and ball milling can be conveniently coupled with PS processing by a micro-flow pump. The overall fabrication process is thereby simplified, by omitting separate wet chemical synthesis steps.

Highly active cathodes are generally composed of three functional layers: electrochemically active layers with fine grain size and good interfacial bonding, diffusion layers with large open porosity, and current collecting layers with high-electronic conductivity. As in the case of anodes, functionally graded or multi-layered cathodes with variations in microstructure and composition are used to increase electrochemical and mechanical performance. Although traditional wet ceramic processing is capable of fabricating these complex electrodes layer by layer, the total process time and cost are high due to repeated coating, drying, and firing. PS processing offers a simple alternative processing technique to fabricate graded or multi-layered structures by the adjustment of the relative flow rates of different feedstocks and of the spraying parameters during coating. Functionally graded cathodes with thicknesses of 40–80 μm can be realized by PS processing. The spraying conditions are ideally selected to deposit the total cathode thickness within five to six layers, each of approximately 10 μm in thickness. Functionally graded cathodes have been prepared and show better electrochemical performance compared with traditional composite cathodes [30].

Despite these potential advantages, PS processing tends to result in fairly dense cathodes with 5–15 vol.% porosity [86]. Due to its higher melting and boiling points, YSZ can prevent over-sintering of sprayed LSM cathodes and thereby increase the porosity of composite layers [43,45,87,88]. By the introduction of carbon or other pore formers to the feedstock, the porosity can also be increased after the pore formers are burned out [31,83]. Fig. 9 shows the effects of pore formers on the porosity of plasma sprayed cathodes [83]. The higher porosity results from the larger volume of void spaces left after pore former removal.

In some cases, needle-shaped single crystals are initially formed in sprayed cathodes that then develop into a columnar microstructure [87]. Open porosity of the needle-shaped electrodes offers efficient vertical as well as horizontal gas migration paths and short electrical current paths. This combination of properties is especially advantageous for application in SOFC electrodes. A columnar cathode fabricated by PS processing is shown in Fig. 10 [87]. Plasma sprayed LSCF cathodes have good contact between the particles, and low polarization resistance values [89]. In contrast, screen-printed cathodes sintered above 1100 °C have larger grains and shorter TPB length.

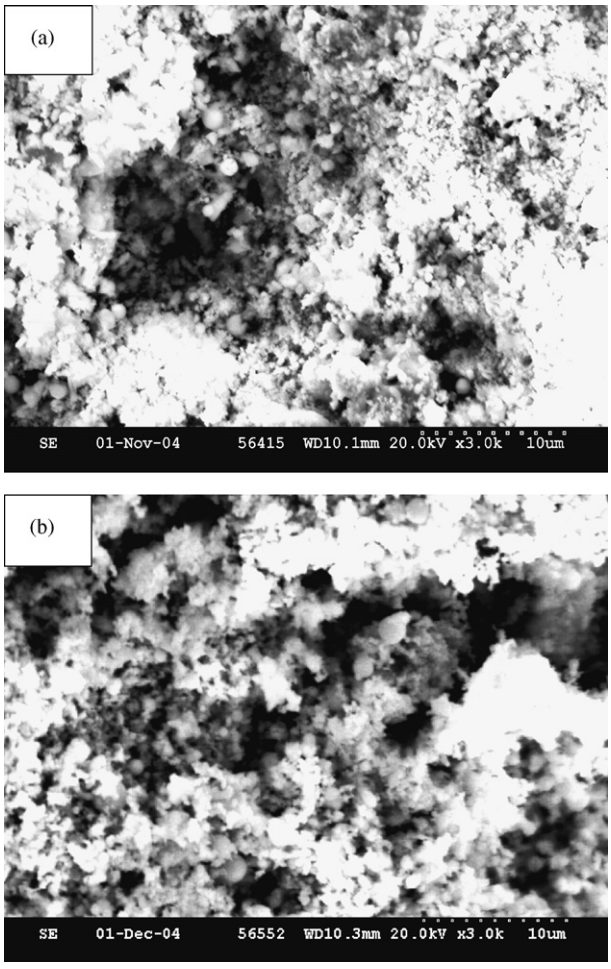

Fig. 9. Effect of pore former concentration on the porosity of a plasma sprayed cathode: (a) 30 vol.% pore former and (b) 40 vol.% pore former [83].

4.5. Interconnect fabrication

PS processing can be used to rapidly fabricate coatings in flexible geometric configurations, thus allowing the deposition

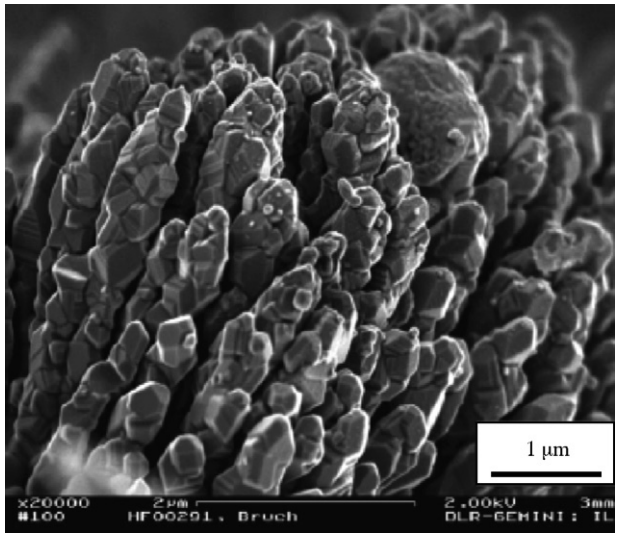

Fig. 10. SEM image of a plasma sprayed LSM coating on a substrate [87].

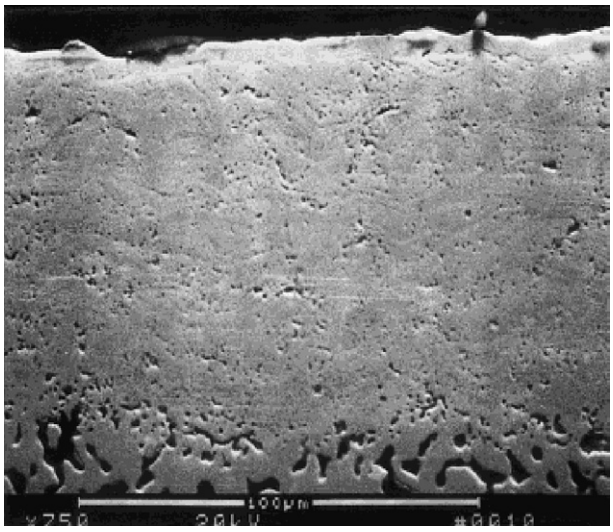

Fig. 11. Microstructure of a heat-treated (1300 °C for 2 h) interconnect [93].

of fully dense interconnect strips on a narrow portion of tubular cells, which would be difficult to achieve through wet ceramic techniques [59,68,90,91]. PS processing is a powerful routine to deposit $LaCrO_3$-based interconnects, but plasma sprayed interconnects are normally porous, and require a heat treatment between 1400 °C and 1550 °C for densification [92]. Such high-temperature treatment is undesirable, due to the significant Mn–Cr inter-diffusion between cathode and interconnect, and due to detrimental effects on the electrode microstructures and on cathode perovskite materials during co-firing of the interconnects with the other cell layers. A novel PS process with calcium aluminate dopant has been developed for the deposition of dense $LaCrO_3$-based interconnect layers [93]. The calcium aluminate additive can facilitate interconnect densification, most likely through the formation of (a) low melting temperature phase(s) in the Ca–Cr–Al–O system. Fig. 11 shows an SEM micrograph of an interconnect layer that was heat treated at approximately 1300 °C [93]. The interconnect is chemically stable under fuel cell operation conditions.

PS has also been used for the fabrication of coatings on interconnect substrate alloys, to protect them from oxidation and to protect the cathodes from chromium evaporation from the interconnect alloys [94–96]. Plasma spray processing is a particularly useful technique for this purpose, due to the ability to coat ceramic coatings that are oxidation resistant and gas tight, without the need for any specialized chemical properties of the coating precursor materials. The technique can also be used to spray coatings on the insides of gas flow channels, provided that the channels are sufficiently angled for access to the spray stream.

5. Integrated fabrication of multiple SOFCs layers

5.1. Integrated fabrication

The use of metallic substrates as SOFC supports has the potential to greatly lower the raw material cost for the stack due to the approximately one order of magnitude lower cost of stainless steel compared to the NiO and YSZ raw materials used for the fabrication of anode support layers. Ceres Power Ltd. has reported that a gadolinia-doped ceria (GDC) thin electrolyte supported on Ti–Nb stabilized 18% Cr ferritic stainless steel can be densified by sintering below 1000 °C in air [97]. Serious metal oxidation, however, can be expected. Another processing route that avoids metal support oxidation is to use ceramic and metal powder processing combined with co-firing on an appropriate metal supported structure in a reducing environment [98]. However, time-intensive procedures for producing functional layers, safety considerations of co-firing in reducing environments, difficulty of binder burnout, and serious inter-diffusion of Cr and Fe from the metallic substrate and Ni from the anode layer at high-sintering temperatures (above 1350 °C) all create obstacles for this processing route.

In contrast, plasma spray processing offers an ideal choice to allow the electrochemically active thin layers of anode, electrolyte, and cathode to be consecutively deposited on a porous metallic (or ceramic) support, resulting in integrated fabrication of SOFCs. In recent years, Westinghouse has been involved in the fabrication of SOFC components through PS processing (Table 2) [71,99]. Integrated fabrication offers the potential for significant performance improvements because all three electrochemically active SOFC components can be fabricated in thin layers, thus decreasing the ohmic resistance and gas diffusion impedance. The integrated fabrication on porous metallic substrates can be completed within several minutes, with no high-temperature post-deposition heat treatment required after plasma spraying. One automated plasma deposition torch can be used to manufacture a much larger volume of cells in a given period of time than with comparable capital equipment investments in wet chemical and firing technologies, thus allowing the production of SOFCs to be scaled up substantially at lower capital cost. This is a significant advantage compared to the wet ceramic processing routes, which require long firing times at high temperatures. Entire 20 cm × 20 cm SOFC cells have been produced by PS processing at the German Aerospace Centre (DLR) [100].

Moreover, the deposition efficiency of raw materials increases with the enlargement of cell size, since almost all of the material is deposited on the cell rather than on surrounding equipment for large cell areas. Consequently, the process is also very cost effective from a material wastage point of view, due to the potential for comparable or even lower material wastage compared with wet ceramic processing. Good adhesion between adjacent layers and therefore low electrical contact resistance can be achieved through PS processing. Using a porous metallic substrate as the cell support, rather than a brittle ceramic layer, also greatly increases the robustness of the stack, which is of great importance for auxiliary power unit (APU) applications in the transportation industry. The smaller thermal mass of metal supported cells compared to ceramic or cermet-supported cells also decreases start-up times, another important factor for transportation applications.

Porous metallic substrate supported SOFCs have been successfully fabricated through integrated APS, with only the LSCF cathode layer being slurry coated [101]. As shown in Fig. 12

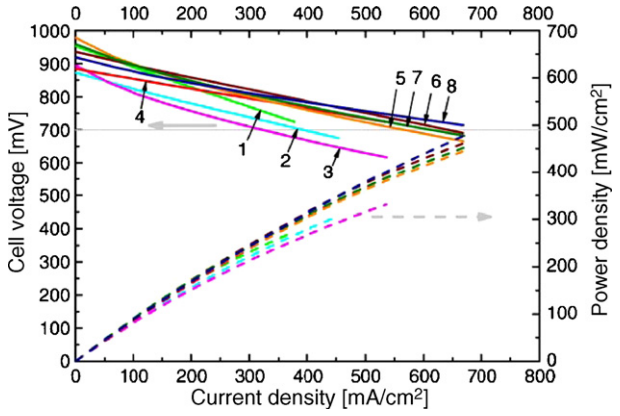

Fig. 12. Cell voltage and power density of APS cells with slurry coated LSCF cathode as a function of current density. The numbers indicate subsequent coating passes [101] (with reproduction permission from Elsevier Ltd.).

[101], a current density of approximately 700 mA cm^{-2} and a power density of 500 mW cm^{-2} at 800 °C have been realized. This technological breakthrough has been achieved by optimizing the hot spraying conditions for microcrack-free coating deposition. The velocity of the spray gun, which controls the local heating of substrate and coating, was also optimized in order to avoid substrate deformation and to achieve dense microstructures. With this additional optimization step, the leakage rates of the coatings could be reduced from about 5–10 mbar l cm^{-2} s for conventionally sprayed YSZ coatings to 0.02 mbar l cm^{-2} s. This improvement in leakage rates is shown in Fig. 13 [101].

A free standing SOFC has been fabricated with a yttrium-doped $SrTiO_3$ (SYT) anode, LSGM electrolyte, and LSM cathode by integrated APS processing. The three active layers were plasma sprayed onto an Al foil layer by layer, and the Al foil was later removed in a basic solution. Fig. 14 shows a typical cross-sectional SEM micrograph of the free standing SOFC. The electrolyte layer is very dense, while cathode and anode

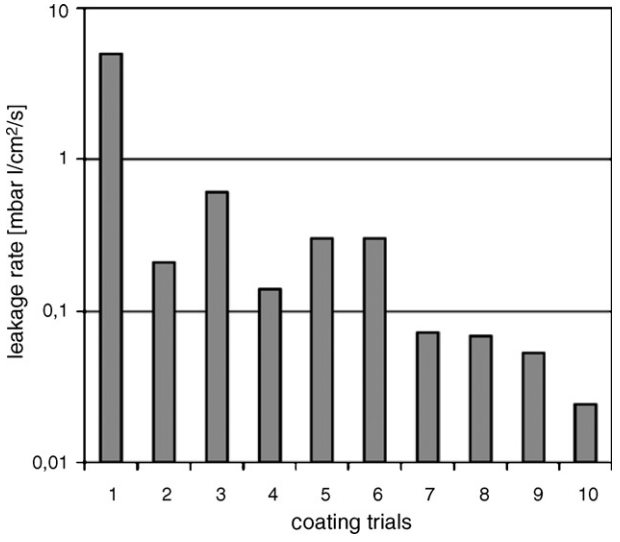

Fig. 13. Leakage rates of electrolyte coatings [101] (with reproduction permission from Elsevier Ltd.).

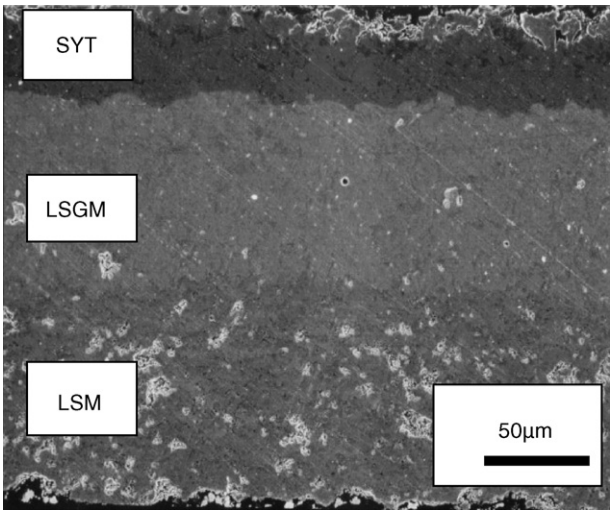

Fig. 14. SEM micrograph of a free-standing SOFC fabricated by plasma spraying [48].

are rather porous. Fig. 15 gives the overall performance of a SOFC single cell using a nanostructured SYT anode, LSGM electrolyte, and LSM cathode. A maximum power density of 85 mW cm^{-2} was achieved at 800 °C. Other factors, including the presence of amorphous phases, composition, and porosity of anode and cathode need to be considered with respect to future improvements of cell performance.

More intensive investigations have been carried out at DLR, where vacuum plasma spraying (VPS) is intensively investigated [102–111]. Carrying out the spraying process in low pressure atmospheres (50–250 mbar) results in longer laminar plasma jets with higher velocities, and reduces interaction with the surrounding cold gas. Powder that is injected into the plasma is accelerated and melted in the fast plasma jet. The coating is formed by solidification and flattening of the fast particles at impact on the substrate. The velocity and degree of melting of the particles can be adjusted by the spraying conditions. This enables the fabrication of either very dense electrolyte layers or of electrode layers with controlled porosity [102].

The main facilities in DLR are three dc plasma installations and two radio frequency (RF) plasma installations, as shown in Fig. 16 [110]. By applying high-velocity Laval nozzles for

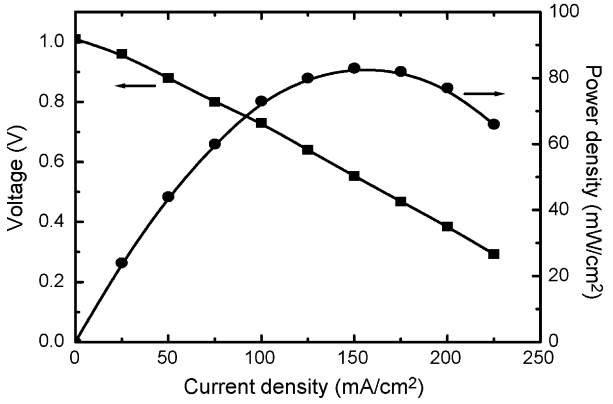

Fig. 15. *I/V* curve of the free-standing cell shown in Fig. 13 [48].

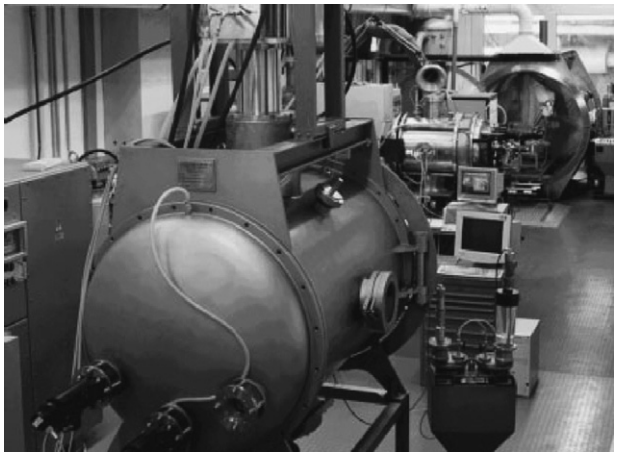

Fig. 16. DLR plasma spray laboratory with dc (background) and RF (foreground) plasma installations [110] (with reproduction permission from John Wiley & Sons Canada, Ltd.).

dc plasma spraying, particle velocities of up to 900 m s^{-1} have been attained [110]. RF plasma spraying using liquid precursors, so-called thermal plasma chemical vapor deposition (TPCVD) processing, is increasingly applied, particularly for the formation of highly porous cathode layers. Fig. 17 [110] presents the principle of the DLR planar thin-film concept of a metallic substrate-supported SOFC based on PS technology. The mechanical strength of the thin-film cell and its excellent electrical and thermal conductivity are provided by an open porous metallic substrate, which also serves as a fuel gas distributor. All functional layers of the cell, anode, electrolyte, and cathode, are deposited onto the porous metal substrate by consecutive VPS layer depositions in a single procedure. The move from a ceramic to a metallic substrate support considerably reduces the problem of crack formation, offering the possibility for large cell sizes and simplified stack design. The development of an appropriate metallic substrate in cooperation with industrial partners is presently a main activity for the realization of the spray concept.

Fig. 18 [110] shows the cross-section of a plasma sprayed SOFC, consisting of a NiO–ScSZ (scandia-stabilized zirconia) anode, ScSZ electrolyte, and LSM–ScSZ cathode. All three layers were consecutively sprayed onto a porous Ni felt. The cell exhibits a dense YSZ electrolyte with lamellar microstructure,

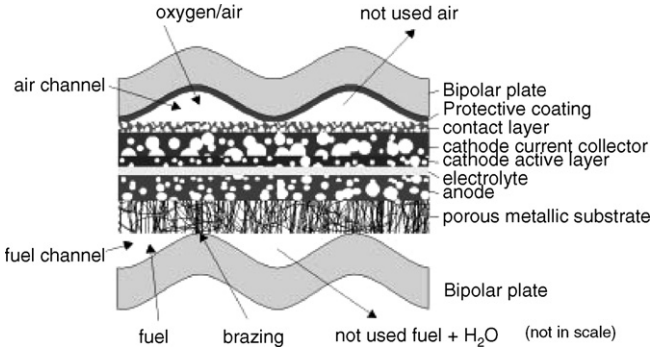

Fig. 17. Principle of planar SOFC design according to the DLR spray concept [110] (with reproduction permission from John Wiley & Sons Canada, Ltd.).

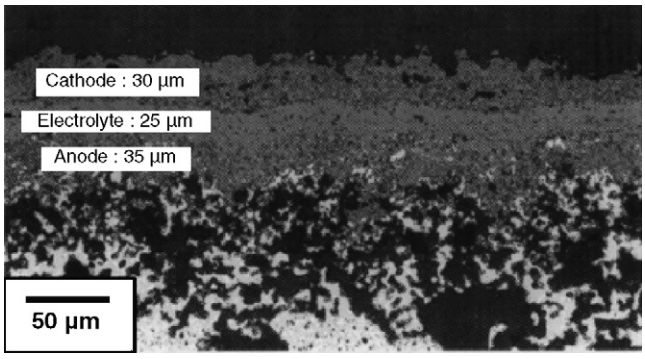

Fig. 18. Cross-section of a vacuum plasma sprayed SOFC [110] (with reproduction permission from John Wiley & Sons Canada, Ltd.).

an anode with a fine open porosity of 21 vol.% after reduction, and a relatively coarsely structured cathode with overall porosity of only approximately 10 vol.%. Fed with H_2 as the fuel gas and oxygen as the oxidant gas, the plasma sprayed cell reached high-power densities of 770 mW cm^{-2} at 900 °C, 590 mW cm^{-2} at 850 °C, 430 mW cm^{-2} at 800 °C, and 290 mW cm^{-2} at 750 °C at a cell voltage of 0.7 V, as shown in Fig. 19 [110]. To further improve cathode porosity, further development focuses on the usage of alternative cathode powders, the application of pore formers, and further optimization of the spray parameters [104].

5.2. Porous metallic substrates for metal-supported SOFCs

For the integrated fabrication of entire SOFCs, porous metallic substrates act not only as structural support and gas distributor, but also have a decisive role in the electrochemical performance of the sprayed cells. The substrate development has turned out to be a key problem in the plasma sprayed SOFC concept. Material requirements for the porous metallic substrates [100,112] include:

(1) high-thermal conductivity;
(2) good corrosion resistance in both oxidizing and reducing atmospheres;

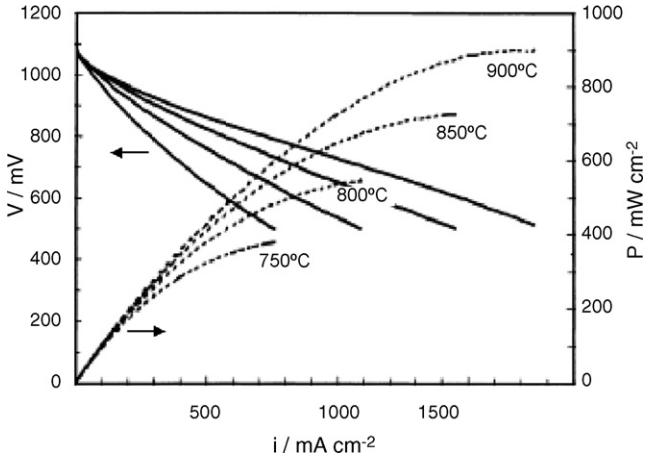

Fig. 19. Electrochemical behavior of a plasma sprayed SOFC plotted in an *I*/*V* graph at different temperatures [110] (with reproduction permission from John Wiley & Sons Canada, Ltd.).

(3) high-electrical conductivity both of the initial material and of oxide scales growing during operation;
(4) good adhesion of oxide scales to initial material;
(5) thermal expansion coefficient should be matched to the other materials in the stack ($\sim 11 \times 10^{-6}\,K^{-1}$, between 30 °C and 1000 °C);
(6) good electrical contact with the cell;
(7) ability to endure thermal cycling;
(8) high porosity and large holes at the interconnect side for gas diffusion;
(9) homogenous fine pores at the electrode side for better interfacial bonding;
(10) high strength;
(11) low cost and easy availability.

Chromium-based, nickel-based, and ferrite-based porous metals have been used as metallic substrates having high-electrical conductivity, good porosity, and reasonably matched TEC with standard SOFC layers, especially the Ni/YSZ anodes [100]. However, no commercially available metal materials can completely satisfy all of the criteria listed above. One of the promising materials is nickel felt, which shows excellent oxidation stability in reducing gas atmospheres. It has been reported [112] that the open circuit voltage of the Ni felt supported cell is lower than that of the cell with the FeCrAlY substrate. The reason might be the higher TEC of Ni (TEC, about $16.0 \times 10^{-6}\,K^{-1}$), which promotes microcracks in the sprayed YSZ thin-film. However, the cell with the Ni felt support achieves much higher power densities due to the higher electrochemical activity of nickel compared with ferritic steel materials, and the disappearance of oxide scales during cell operation [109,113,114]. Moreover, the inherent flexibility of the felt structure can compensate the TEC mismatch with the sprayed cell layers to a certain extent [100]. Recent results show that relatively dense electrolyte structures can be fabricated [114]. However, nickel felt shows a strong post-processing sintering effect and is significantly compressed during long-term operation, resulting in significant cell degradation. Moreover, nickel substrates are more expensive than ferrite-based steel foams.

For most ferritic steels, oxidation is a serious problem at SOFC operation conditions and has been widely investigated (e.g. [115,116]). For porous metallic interconnects acting as substrates for entire cells, the oxidation behavior is much more complicated and serious because of the much higher surface/volume ratio of the porous structure compared to that of dense interconnects with machined gas flow channels.

The surface roughness of the metallic support layers must be considered in the deposition of SOFC layers. The surface roughness of plasma sprayed layers is dependent on the substrate surface roughness, and is also highly dependent on initial feedstock particle size and on spraying conditions, particularly the extent of melting. By using finer particles during spraying, the surface roughness of PS layers can be reduced, even when initially deposited on a rougher substrate.

6. Challenges and conclusions

Despite the potential benefits that some of plasma spray processing can offer, such as the cost-effective production of high-performance SOFCs, significant challenges still remain in the development of PS processing with respect to the state of the art SOFC wet ceramic production techniques. PS coatings currently manufactured for common applications such as thermal barrier coatings typically exhibit porosities in the range of 5–15 vol.%. For the successful application of PS in SOFC fabrication, this range must be extended down to less than 5 vol.% open porosity for dense electrolytes, and up to ~40 vol.% for porous electrodes, particularly on the cathode side where no post-deposition porosity can be introduced by reduction of NiO to Ni, as on the anode side. The process must also be controlled to ensure that the phases deposited have the desired crystalline structure, avoiding delamination, amorphous structures, and to avoid introducing impurities in the raw materials during powder preparation, or in the cell during PS processing. Typical in-plane splat orientations, although beneficial for tubular cells, are less conducive to ideal electrical performance in planar cells due to inter-lamellar cracks and pores. Furthermore, manufacturing of SOFCs by PS processing will also require procedures to be developed that increase product thermal shock resistance during processing. Use of metallic interconnect substrates rather than ceramic supports partly alleviates this problem. Optimized control of substrate heating and cooling can also minimize the effects of thermal stresses during the deposition process. Finally, over-spraying should be continuously minimized to reduce material waste. A system and procedure for the collection and recycling of over-sprayed materials may be required in future development.

While cost and performance of SOFCs remain major barriers to their more widespread use, PS processing has the potential to drastically reduce these barriers by rapidly increasing production rates and reducing capital equipment, materials, and SOFC system costs. Plasma spraying also has the potential to increase performance by the use of graded compositions and microstructures, and by rapidly solidifying fine microstructures with good adhesion to the substrates and no microstructural coarsening due to sintering. However, several important challenges have to be solved before the full potential of the advantages of the PS technique can be realized. Numerous research efforts are currently underway to address these challenges, with the goal of accelerating the worldwide commercialization of SOFCs.

Acknowledgments

The authors gratefully acknowledge financial support from the National Fuel Cell and Hydrogen Program of the National Research Council Canada and Northwest Mettech Corporation.

References

[1] M.C. Williams, J. Strakey, W. Surdoval, J. Power Sources 159 (2006) 1241–1247.
[2] R.J. Gorte, J.M. Vohs, S. McIntosh, Solid State Ionics 175 (2004) 1–6.

[3] O. Kesler, M. Finot, S. Suresh, S. Sampath, Acta Mater. 45 (1997) 3123–3134.
[4] O. Kesler, J. Matejicek, S. Sampath, S. Suresh, T. Gnaeupel-Herold, P.C. Brand, H.J. Prask, Mater. Sci. Eng. A 257 (1998) 215–224.
[5] P. Fauchais, G. Montavon, M. Vardelle, J. Cedelle, Surf. Coat. Technol. 201 (2006) 1908–1921.
[6] M. Moss, D.L. Smith, R.A. Lefever, Appl. Phys. Lett. 5 (1964) 120–121.
[7] P. Fauchais, J.F. Coudert, M. Vardelle, A. Vardelle, A. Denoirjean, J. Therm. Spray Technol. 1 (1992) 117–128.
[8] J.F. Coudert, M.P. Planche, P. Fauchais, Plasma Chem. Plasma Process 15 (1995) 47–70.
[9] S.C. Snyder, L.D. Reynolds, J.R. Fincke, G.D. Lassahn, J.D. Grandy, T.E. Repetti, Phys. Rev. E: Stat. Phys. Plasmas Fluids Relat. Interdisc. Topics 50 (1994) 519–525.
[10] P. Fauchais, J. Phys. D: Appl. Phys. 37 (2004) R86–R108.
[11] J. Cedelle, M. Vardelle, P. Fauchais, Surf. Coat. Technol. 201 (2006) 1373–1382.
[12] H. Bhat, H. Hermann, Proceedings of the International Conference on Metallurg. Coat. Proc. Technology, San Diego, CA, USA, April 5–8, 1982, pp. 227–234.
[13] P. Fauchais, A. Vardelle, B. Dussoubs, J. Therm. Spray Technol. 10 (2001) 44–66.
[14] Y.Y. Zhao, P.S. Grant, B. Cantor, J. Microscopy 169 (1993) 263.
[15] C. Challener, Chem. Market Rep. 263 (2003) 1–4.
[16] S. Hui, A. Petric, J. Electrochem. Soc. 149 (2002) J1–J10.
[17] B.H. Kear, P.R. Strutt, Naval Rev. XLVI (1994) 4.
[18] H. Gleiter, Nanostruct. Mater. 1 (1992) 1–9.
[19] C.G. Granquist, R.A. Buhman, J. Appl. Phys. 47 (1976) 2200.
[20] M.L. Lau, H.G. Jiang, R.J. Perez, J. Juarez-Islas, E.J. Lavernia, Nanostruct. Mater. 9 (1997) 157–160.
[21] M.L. Lau, H.G. Jiang, R.J. Perez, J. Juarez-Islas, E.J. Lavernia, Nanostruct. Mater. 7 (1996) 847–856.
[22] T.D. Xiao, K.E. Gonsalves, P.R. Strutt, P.G. Klemens, J. Mater. Sci. 28 (1993) 1334–1340.
[23] J. Schoonman, Solid State Ionics 135 (2000) 5–19.
[24] Q. Zhu, B. Fan, Solid State Ionics 176 (2005) 889–894.
[25] Himeko Ohrui, Toshio Matsushima, Toshiro Hirai, J. Power Sources 71 (1998) 185–189.
[26] E.J. Lavernia, US Patent 5,939,146 (1999).
[27] J.C.C. Chen, H. Chen, R. Prasad, G. Whichard, US Patent 6,638,575 (2003).
[28] R. Goswami, S. Sampath, J. Parise, H. Herman, US Patent 6,258,417 (2001).
[29] Z. Tang, A. Burgess, O. Kesler, B. White, N. Ben-Oved, Proceedings of the International Therm. Spray Conference, Beijing, China, 2007.
[30] K. Barthel, S. Rambert, Proceedings of the 5th International Symposium Functionally Graded Materials (FGM 98), Dresden, Germany, 1998, pp. 800–805.
[31] L. Tai, P.A. Lessing, J. Am. Ceram. Soc. 74 (1991) 501–504.
[32] S. Hui, X. Ma, H. Zhang, H. Chen, J. Roth, J. Broadhead, A. Decarmine, M. Wang, T. Xiao, International Patent, 2003, WO 03/075383 A2.
[33] S. Hui, H. Zhang, J. Dai, X. Ma, T.D. Xiao, D.E. Reisner, Proceedings of the 8th International Symposium on Solid Oxide Fuel Cells (SOFC-VIII), Paris, France, April 27–May 2, 2003.
[34] S. Hui, H. Zhang, X. Ma, J. Roth, T.D. Xiao, D.E. Reisner, Progress Report: Sequential-Fab Plasma-Sprayed Components for Intermediate Temperature SOFCs Fuel Cell 2003—Proceedings of the Third Annual BCC Conference: Connections to Commercialism, Stamford, CT, USA, March 31–April 1, 2003.
[35] S. Hui, J. Dai, J. Roth, D. Xiao, Fabrication of Nanostructured Components with High Porosity Using Plasma Spray, 2002 MRS Fall Meeting, Boston.
[36] G. Schiller, R. Henne, M. Lang, M. Muller, Mater. Sci. Forum Pt. 3 (2003) 2539–2544.
[37] F. Gitzhofer, M. Boulos, J. Heberlein, R. Henne, T. Ishigaki, T. Yoshida, MRS Bull. 25 (2000) 38–42.
[38] R. Henne, M. Lang, M. Muller, G. Schiller, Czech. J. Phys. 52 (2002) D896–D904.
[39] G. Schiller, R. Henne, M. Lang, Proceedings of the 5th International Symposium on SOFC–SOFC V, 1997, pp. 635–644.
[40] J. Musil, M. Alaya, R. Oberacker, J. Thermal Spray Technol. 6 (1997) 449–455.
[41] M.E. Bonneau, F. Gitzhofer, M.I. Boulos, Proceedings of the International Thermal Spray Conference Expo. (ITSC'2000), Montreal, Canada, 2000.
[42] E. Theophile, F. Gitzhofer, M.I. S Boulos, Manufacturing of solid oxide fuel cells components by induction plasma spraying UTSC'99 – Proceedings of the 2nd United Thermal Spray Conference Exposition – Coating in Practice, Dusseldorf, Germany, 1999.
[43] B.D. White, O. Kesler, Adv. Mater. Res. 15–17 (2007) 299–304.
[44] N. Ben Oved, O. Kesler, Adv. Mater. Res. 15–17 (2007) 287–292.
[45] B.D. White, O. Kesler, N. Ben-Oved, A. Burgess, Proceedings of the International Thermal Spray Conference, Seattle, WA, May, 2006.
[46] T. Chraska, A.H. King, C.C. Berndt, J. Karthikeyan, MRS Symp. Proc. Mater. Res. Soc. 481 (1998) 613.
[47] S. Pirzada, T. Yadav, US Patent 5,851,507 (1998).
[48] Authors' previously unpublished work.
[49] Z. Wang, R. Hui, N. Bogdanovic, Z. Tang, S. Yick, I. Yaroslavski, A. Burgess, R. Maric, D. Ghosh, J. Power Sources, in press.
[50] L. Rose, M. Menon, P.H. Larsen, J. Danish Ceram. Soc. 18 (2006) 16.
[51] X. Zhang, S. Ohara, H. Okawa, R. Maric, T. Fukui, Solid State Ionics 139 (2001) 145.
[52] O. Kesler, Mater. Sci. Forum v539–543 (2007) 1385–1390.
[53] A.E. Giannakopoulos, S. Suresh, M. Finot, M. Olsson, Acta Mater. 43 (1995) 1335–1354.
[54] R.J. Gorte, S. Park, J.M. Vohs, C. Wang, Adv. Mater. 12 (2000) 1465–1469.
[55] S. Tao, J.T.S. Irvine, J. Electrochem. Soc. 151 (2004) A252–A259.
[56] J. Vulliet, B. Morel, J. Laurencin, G. Gauthier, L. Bianchi, S. Giraud, J.Y. Henry, F. Lefebvre-Joud, Electrochem. Soc. Proc. 07 (2003) 803–811.
[57] C. Iwasawa, M. Nagata, N. Kaneta, Y. Seino, M. Ono, Proceedings of the 5th International Symposium on SOFC–SOFC V, Aachen, Germany, 1997, pp. 626–634.
[58] T. Kato, S. Wang, A. Negishi, S. Nagata, K. Nozaki, Proceedings of the 4th Eur. SOFC Forum, vol. 2, 2000, pp. 553–560.
[59] Y. Ohno, Y. Kaga, S. Nagata, Trans. Inst. Elect. Eng. Jpn. 107 (1) (1987) 59–67.
[60] H. Yokokawa, Proceedings of the 6th International Conference on Solid Oxide Fuel Cells, PV99-19, 1999, pp. 10–18.
[61] L. Rose, O. Kesler, Z. Tang, A. Burgess, J. Power Sources 167 (2007) 340–348.
[62] K.A. Khor, L.-G. Yu, S.H. Chan, X.J. Chen, J. Eur. Ceram. Soc. 23 (2003) 1855–1863.
[63] S. Oh, T. Otagawa, M. Madou, Proceedings of the 27th Intersociety Energy Conv. Eng. Conf., IEEE Cat. No. 92CH3164-1, vol. 3, San Diego, CA, August 3–7, 1992, pp. 3401–3406.
[64] R. Vaßen, D. Hathiramani, R.J. Damani, D. Stöver, Electrochem. Soc. Proc. 07 (2005) 1016–1024.
[65] K.W. Schlichting, N.P. Padture, P.G. Klemens, J. Mater. Sci. 36 (2001) 3003–3010.
[66] M. Scagliotti, F. Parmigiani, G. Samoggia, G. Lanzi, D. Richon, J. Mater. Sci. 33 (1988) 3764–3770.
[67] C. Li, C. Li, X. Ning, Vacuum 73 (2004) 699–703.
[68] O. Takayasu, K. Yasuo, M. Akihiko, Bull. Electrotech. Lab. 60 (2) (1996) 1–9.
[69] T. Okuo, Y. Kaga, A. Momma, A. Denki Kagaku oyobi Kogyo Butsuri Kagaku, 64 (6) (1996) 555–561.
[70] T. Okuo, S. Nagata, Y. Kaga, Y. Kasuga, A. Momma, K. Tsukamoto, F. Uchiyama, Proceedings of the 1st European SOFC Forum, vol. 2, 1994, pp. 909–918.
[71] G. DiGiuseppe, Electrochem. Soc. Proc. 07 (2005) 322–333.
[72] P. Fauchais, V. Rat, C. Delbos, J.F. Coudert, T. Chartier, L. Bianchi, IEEE Trans. Plasma Sci. 33 (2005) 920–930.
[73] J.O. Berghaus, J.G. Legoux, C. Moreau, R. Hui, D. Ghosh, Thermec' 2006. International Conference Proceedings of Manu. Adv. Mater. 2006, Vancouver, BC, Canada, p. 92.

[74] J. Karthikeyan, C.C. Berndt, J. Tikkanen, S. Reddy, H. Herman, Mater. Sci. Eng. A 238 (1997) 275–286.
[75] Y. Mizoguchi, M. Kagawa, M. Suzuki, Y. Syono, T. Hirai, Nanostruct. Mater. 4 (5) (1994) 591–596.
[76] C. Monterrubio-Badillo, H. Ageorges, T. Chartier, J.F. Coudert, P. Fauchais, Surf. Coat. Technol. 200 (2006) 3743–3756.
[77] J.R. Mawdsley, Y. Jennifer Su, K.T. Faber, T.F. Bernecki, Mater. Sci. Eng. A 308 (2001) 189–199.
[78] D.E. Boss, T. Bernecki, D. Kaufman, S. Barnett, Proceedings of the Fuel Cell'97 Review Meeting, Morgantown, West Virginia, August 26–28, 1997.
[79] M. Backhaus-Ricoult, Annu. Rev. Mater. Res. 33 (2003) 55–90.
[80] J.A.M.V. Roosmalen, E.H.P. Cordfunke, Solid State Ionics 52 (1992) 303–312.
[81] L. Rose, M. Menon, K. Kammer, O. Kesler, P.H. Larsen, Adv. Mater. Res. 15–17 (2007) 293–299.
[82] R. Zheng, X.M. Zhou, S.R. Wang, T.-L. Wen, C.X. Ding, J. Power Sources 140 (2005) 217–225.
[83] J. Jankovic, S.R. Hui, J. Roller, O. Kesler, Y. Xie, R. Maric, D. Ghosh, COM 2005. Proceedings of the Canadian Conference on Metallurg., Calgary, Alberta, Canada, 2005.
[84] G. Schiller, M. Müller, R. Henne, 48. Intemationales Wissenschaftliches Kolloquium, Technische Universitat Ilmenau, Ilmenau, Germany, September 22–25, 2003.
[85] M. Nikravech, F. Rousseau, D. Morvan, J. Amouroux, J. Phys. Chem. Solids 64 (2003) 1771–1775.
[86] G. Schiller, M. Müller, F. Gitzhofer, J. Therm. Spray Technol. 8 (1999) 389–392.
[87] M. Müller, E. Bouyer, M.V. Bradke, D.W. Branston, R.B. Heimann, R. Henne, G. Lins, G. Schiller, Materialwiss. u. Werkstofftech. 33 (6) (2002) 322–330.
[88] S. Rambert, A.J. McEvoy, K. Barthel, J. Eur. Ceram. Soc. 19 (1999) 921–923.
[89] D. Bouchard, L. Sun, F. Gitzhofer, G. Brisard, Electrochem. Soc. Proc. 07 (2003) 330–331.
[90] H. Mori, H. Omura, N. Hisatome, K. Ikeda, K. Tomida, SOFC VI—Proceedings of the 6th International Symposium, 1999, pp. 52–59.
[91] M. Nagata, C. Iwasawa, S. Yamaoka, Y. Seino, M. Ono, Proceedings of the 4th International Symposium SOFC–SOFC-IV, 1995, pp. 173–179.
[92] J.H. Kim, R.H. Song, K.S. Song, S.H. Hyun, D.R. Shin, H. Yokokawa, J. Power Sources 122 (2003) 138–143.
[93] L.J.H. Kuo, S.D. Vora, S.C. Singhal, J. Am. Ceram. Soc. 80 (1997) 589–593.
[94] E. Fendler, R. Henne, R. Ruckdaschel, H. Schmidt, Proceedings of the 2nd Eur. SOFC Forum Proc., pt. 1, vol. 1, 1996, pp. 269–277.
[95] G. Schiller, R. Henne, R. Ruckdaeschel, J. Adv. Mater. 32 (1) (2000) 3–8.
[96] E. Batawi, K. Honegger, R. Diethelm, M. Wettstein, Proceedings of the 2nd Eur. SOFC Forum, Pt. 1, vol. 1, 1996, pp. 307–314.
[97] P. Attryde, A. Baker, S. Baron, A. Blake, N.P. Brandon, D. Corcoran, D. Cumming, A. Duckett, K. El-Koury, D. Haigh, M. Harrington, C. Kidd, R. Leah, G. Lewis, C. Matthews, N. Maynard, T. McColm, A. Selcuk, M. Schmidt, R. Trezona, L. Verdugo, Electrochem. Soc. Proc. 07 (2005) 112–122.
[98] S.J. Visco, C.P. Jacobson, I. Villareal, A. Leming, Electrochem. Soc. Proc. 16 (2003) 1040–1050.
[99] J. Brogan, R. Gambino, R. Greenlaw, J. Gutleber, S. Toth, Office of Fossil Energy Fuel Cell Program FY 2004 Annual Report, VII.10 Adv. Thermal Spray Fabric. Solid Oxide Fuel Cells, 2004, pp. 294–298.
[100] G. Schiller, T. Franco, R. Henne, M. Lang, R. Ruckdaschel, Electrochem. Soc. Proc. 16 (2001) 885–894.
[101] D. Stöver, D. Hathiramani, R. Vaßen, R.J. Damani, Surf. Coat. Technol. 201 (2006) 2002–2005.
[102] M. Lang, M. Bilgin, R. Henne, S. Schaper, G. Schiller, Proceedings of the 3rd Euro. SOFC Forum, Nantes, France, 1998, pp. 161–170.
[103] G. Schiller, R. Henne, M. Lang, S. Schaper, Electrochem. Soc. Proc. 19 (1999) 893–903.
[104] G. Schiller, R.H. Henne, M. Lang, R. Ruckdäschel, S. Schaper, Fuel Cell Bull. 3 (2000) 7–12.
[105] M. Lang, T. Franco, R. Henne, S. Schaper, G. Schiller, Proceedings of the 4th Euro. SOFC Forum, Lucerne, Switzerland, 2000, pp. 231–240.
[106] M. Lang, R. Henne, S. Schaper, G. Schiller, J. Therm. Spray Technol. 10 (2001) 618–625.
[107] M. Lang, T. Franco, G. Schiller, N. Wagner, J. Appl. Electrochem. 32 (2002) 871–874.
[108] M. Lang, T. Franco, R. Henne, G. Schiller, S. Ziehm, Fuel Cell Seminar, vol. 11, FL, USA, 2003, pp. 794–797.
[109] G. Schiller, T. Franco, R. Henne, M. Lang, P. Szabo, Electrochem. Soc. Proc. 07 (2003) 1051–1058.
[110] G. Schiller, R. Henne, M. Lang, M. Müller, Fuel Cells 4 (2004) 56–61.
[111] G. Schiller, T. Franco, M. Lang, P. Metzger, A.O. Störmer, Electrochem. Soc. Proc. 07 (2005) 67–75.
[112] T. Franco, R. Henne, M. Lang, P. Metzger, G. Schiller, P. Azabo, S. Ziehm, Electrochem. Soc. Proc. 07 (2003) 923–931.
[113] M. Lang, T. Franco, R. Henne, P. Metzger, G. Schiller, S. Ziehm, Electrochem. Soc. Proc. 07 (2003) 1059–1067.
[114] T. Franco, Z. Ilhan, M. Lang, G. Schiller, P. Szabo, Electrochem. Soc. Proc. 07 (2005) 344–352.
[115] J.W. Fergus, Mater. Sci. Eng. A 397 (2005) 271–283.
[116] W. Qu, L. Jian, D.G. Ivey, J.M. Hill, J. Power Sources 157 (2006) 335–350.